Thermal and UV Degradation of Polymer Films Studied In situ with ESR Spectroscopy

Kenneth Rasmussen,*,† Guenter Grampp,† Marc van Eesbeek,‡ and Thomas Rohr‡

Institute of Physical and Theoretical Chemistry, Graz University of Technology, Technikerstrasse 4/I, 8010 Graz, Austria, and Materials Space Evaluation & Radiation Effects Section, European Space Agency-European Space Research and Technology Centre (ESA-ESTEC), P.O. Box 299, 2200 AG Noordwijk ZH, The Netherlands

ABSTRACT Thermal and UV degradation of four common space-grade polymer films have been studied in situ using electron spin resonance (ESR) spectroscopy. By recording subsequent spectra at a sufficient rate, the time dependence of the radical concentration could be followed, allowing more detailed study of the kinetics of the degradation process. The thermal degradation was found to consist of two main processes, one being a stabilization process and the other the actual degradation, whereas the UV experiments showed biexponential degradation kinetics. Additionally, to compare in situ and ex situ experiments, we monitored the stability of the generated radicals after the exposure. The radical concentration decreased only slightly when samples were stored in a vacuum, whereas storage in air led to a significant loss of radicals.

KEYWORDS: polymer degradation • polyimides • electron spin resonance • degradation kinetics • UV irradiation • thermal aging, space environment

INTRODUCTION

With the current development pace of new polymers having a potential for space applications, a fast screening and cost-effective method for preselection and basic performance characterization would be very valuable. One possible method shall be presented, and its general feasibility demonstrated.

The main method of analysis is ESR spectroscopy (1), which deals with the resonant microwave absorption of samples in an external magnetic field. It is similar to the better known nuclear magnetic resonance (NMR) spectroscopy, but is restricted to paramagnetic compounds, such as organic radicals, complexes of transition metal ions, and defects in crystals. This limitation, however, is also one of the strengths of the method, as it can be applied very specifically.

ESR spectroscopy may be used to determine the amount of spins present in a sample and most often this is done by comparing the double integral attributable to an unknown sample to that of a known standard (2). The reason for this is that the magnitude of the ESR absorption depends heavily on spectrometer settings, as well as on temperature. Furthermore, ESR spectroscopy may provide information about the general type of radicals present, and sometimes their structure, if sufficient hyperfine interactions can be detected.

The idea of using ESR to study polymer degradation is not new and several investigations are reported in literature. Free radicals present in polymers can take part in their degradation, as shown by Ahn and co-workers who studied the behavior of thermally aged polyimide PMR-15 and characterized the generated radicals using conventional ESR (3, 4) as well as ESR imaging (5). Radicals were formed both in nitrogen atmosphere and air and the authors correlated the radical concentration with mass loss experiments and showed that the free radicals are involved in the thermo-oxidation of the polyimides.

In a more recent report, Iwata (6) studied irradiated polyimide films and linked their observed discoloration to the presence of free radicals. A very good correlation was found between the radical concentration and the increase in the absorbance of the materials.

The UV degradation of Kapton H was reported by George et al. (7), who studied samples that had been irradiated in either vacuum or air. These authors, among other things, investigated the dependence of the ESR signal on the duration of irradiation as well as on elevated temperatures, and the stability of the generated radicals was studied. Additionally, they determined the relaxation parameters of the radicals.

Other methods that have been used to generate radicals for use in ESR studies of polyimide degradation include γ-radiolysis (8, 9) and irradiation with accelerated protons (10), electrons (6, 11),and heavy ions (12).

Most of these, however, were conducted ex situ, that is, the sample was exposed to a source of degradation and subsequently transferred to the ESR spectrometer for measurement. An exception is the study of the UV degradation of Kapton, along with a series of other polyimides, conducted by Hill et al. (13). Here samples were irradiated in situ in the ESR resonator and the change in radical concentration with time was monitored.

* Corresponding author. E-mail: Kenneth.Rasmussen@tugraz.at.
Received for review March 14, 2010 and accepted June 5, 2010
† Graz University of Technology.
‡ ESA-ESTEC.
DOI: 10.1021/am100219z

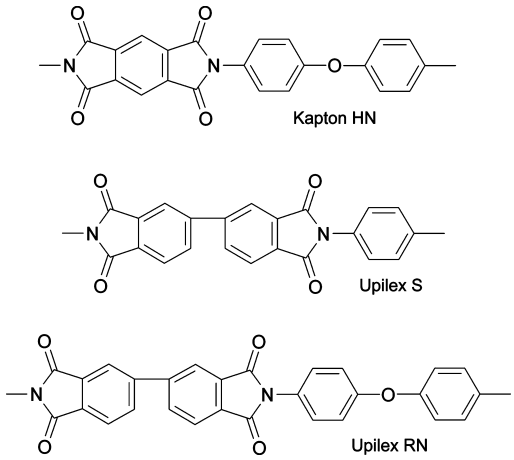

FIGURE 1. Chemical structures of the polyimide units.

In the present work, the radicals created during the thermal or UV degradation of four space-grade polymer films have been monitored during the exposure, thus providing in situ information of the ongoing processes. This provides an opportunity to study the degradation kinetics and to compare with ex situ experiments.

EXPERIMENTAL SECTION

Materials. The materials that were investigated were the polyimides Kapton HN (DuPont, USA), Upilex S and Upilex RN (both UBE Industries, Japan), for which the chemical structures are shown in Figure 1, as well as a fluorinated ethylene propylene copolymer FEP-C (DuPont, USA), all being widely used in the space industry.

Sample Preparation. For the ESR investigations, films in pieces of approximately 10−15 mm width and 30−40 mm length were used. Most films were 25 μm thick, but in the case of Kapton films of thickness 50 and 75 μm were also investigated. Samples were rolled up and introduced into a 6 mm diameter quartz ESR cell and prior to measurements the sample was evacuated and kept under a vacuum for at least an hour before being exposed to elevated temperature or UV irradiation.

ESR Measurements. For the ESR investigations a Bruker EMX ESR spectrometer, operating at 9.5 GHz (X-band) with a 100 kHz modulation frequency, was used. The standard TE 102 mode resonator was installed, with both optical window and cooling plates mounted. A Bruker temperature controller provided the desired temperatures with an accuracy of 1 K. UV-irradiation was provided by a 1000 W mercury/xenon lamp (Newport/Oriel) that was placed in front of the ESR magnet and focused onto the sample using two adjustable lenses. The lamp system and the custom built ESR sample cells that were used have been described elsewhere (14). This reference also contains detailed information on experiment conditions and procedures.

The thermal degradation experiments lasted as long as 120 h, whereas the typical duration of an UV experiment was 30 min. During these, complete ESR spectra were acquired at regular intervals and subsequently analyzed.

Data Analysis. ESR spectra were simulated using noncommercial software (15), yielding the typical ESR parameters. Spin concentrations were determined by double integration of the spectra. These were then related to a spectrum of a Bruker Strong Pitch standard sample of known concentration (14). Note that since it has been established that the radicals generated by UV irradiation are situated close to the surface of the films (7), the concentration unit of spins/cm^2 was preferred in order to facilitate comparisons between films of different thickness.

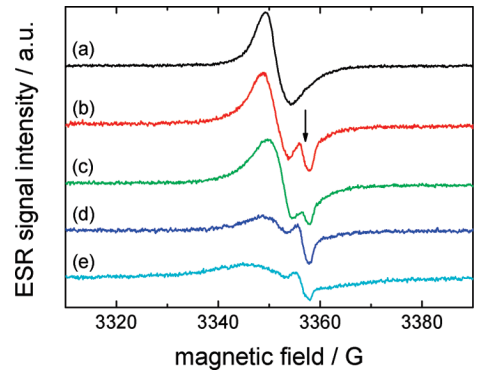

FIGURE 2. ESR spectra of (a) Kapton HN exposed to 573 K for 6 h as well as (b) Kapton HN, (c) Upilex S, (d) Upilex RN, and (e) FEP-C after 30 min of UV irradiation. Spectra were acquired in vacuum at 298 K immediately after end of exposure. The marked signal in b−e is attributable to defects in the quartz sample cell.

Also, for comparisons between the thermal and UV experiments, it should be mentioned that the former are likely to underestimate the actual concentrations because of the sample size. The relatively long samples extend into the less sensitive parts of the ESR resonator meaning that the "effective" area is less than that of the entire sample. On the other hand, by ensuring that the sensitive part of the resonator is completely filled, issues with sample positioning having an effect on the results are avoided.

The obtained results were further investigated, providing curve fits as well as statistical analyses. In most cases, the corrected double integral, $A(t) - A(0)$, was plotted against time before fits to different theoretical models were made. Here the used sample size does not influence the analysis.

RESULTS AND DISCUSSION

ESR Spectra. Typical ESR spectra obtained after the degradation experiments are shown in Figure 2. Pristine samples of Kapton HN and Upilex S show an inherent ESR signal, due to the manufacturing process of the materials, which includes a curing period at elevated temperatures. The Kapton ESR signal showed a single line at $g = 2.005$ with a width of $\Delta B_{pp} = 7$ G, which is in good agreement with literature, reporting $g = 2.005$ and $\Delta B_{pp} = 8$ G (7, 12). For Upilex S, a single line at $g = 2.005$ with a 6 G width was obtained. Thermally and UV-exposed Kapton HN showed a slight line narrowing, whereas the spectrum of Upilex S was not affected by exposure. UV irradiated Upilex RN showed $g = 2.004$ and $\Delta B_{pp} = 9$ G. The obtained g-values are consistent with radicals which are delocalized on ring systems containing oxygen or nitrogen atoms (7, 13), but from the ESR data, it is not possible to determine more detailed structures nor to assign the initial bond cleavage. However, George et al. (7) have suggested the cleavage of the imide linkage as a possible initial step because the C−N bond is comparatively weak.

For FEP-C, an ESR signal with g = 2.003 and $\Delta B_{pp} = 15$ G was found, which corresponds to carbon centered radicals. In a few of the most intense spectra obtained for FEP, shoulders could be detected on the main ESR line but it was not possible to discern whether these originated from fluorine hyperfine splittings or from radical fragments with slightly shifted g values. For comparison, it can be noted that

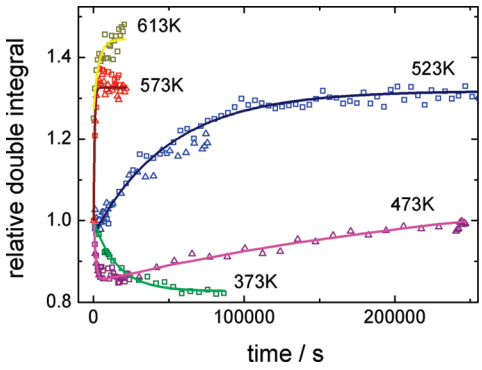

FIGURE 3. Kinetic traces for the thermal decomposition of Kapton HN.

Hill et al. (16), who used γ-radiolysis to generate radicals in powdered FEP, in many cases observed several radical species. For the principal spectrum they report a g value of 2.003 and a line width of approximately 10 G, albeit for spectra recorded at 77 K. Additional ESR data for all four polymers can be found in the Supporting Information together with spectra recorded during exposure.

For all materials the lines deviate from the theoretical Lorentzian and Gaussian line shapes, indicating some degree of unresolved hyperfine splittings, again suggesting delocalized radicals.

In all spectra of UV exposed materials, a narrow signal originating from radiation induced defects in the quartz of the sample cells was observed. This however, did not influence the data analysis (14) and the defects were removed by tempering of the cells between experiments.

Thermal Degradation. All three polyimides were submitted to elevated temperatures, but even at 573 K, only Kapton HN showed noticeable signs of degradation. This observation is in agreement with previously reported mass loss measurements (17, 18).

Assuming that the radicals are formed uniformly in the Kapton film, a concentration at the end of exposure may be calculated, arriving at 3.1×10^{17} radicals g^{-1} for the samples that were kept in vacuum at 573 K for 6 h. For comparison, the PMR-15 samples of Ahn et al. showed a concentration of 6.3×10^{18} radicals g^{-1} (3) in a sample that had been aged in air at 589 K for 16 h.

Kinetic curves are shown in Figure 3 and as can be seen, the behavior of Kapton HN is very different at the various temperatures. Note that here, not the corrected but the relative double integral is plotted. This is done in order to allow a better representation of the curves. Because the ESR absorption depends inversely on temperature, following a Curie–Weiss type law, direct comparison of double integrals attributable to two different temperatures is not straightforward. The shown fits were determined using the original data and normalized correspondingly.

At relatively low temperatures (373 K), a first-order decay described the data well, whereas at high temperatures (above 523 K), the data could be fitted to first-order build ups. At 473 K, it is clear that none of the two situations alone will describe the data sufficiently. However, using the sum of one of each kind of function, a reasonably good fit was obtained. The outcome is shown in Table 1, where k_1 denotes the rate constant of the degradation process and k_2 that of the radical decay. Table 1 also shows the change in spin concentration throughout the experiments and was calculated by comparing room temperature (298 K) spectra recorded before and immediately after exposure. The radical concentration before experiments averaged 1.1×10^{14} spins cm^{-2}.

Table 1. Experimental Rate Constants and Changes in Radical Concentrations (Δc) for Thermally Induced Degradation Experiments on 25 μm Kapton HN Films

T (K)	k_1 ($\times 10^{-5}$ s^{-1})	k_2 ($\times 10^{-5}$ s^{-1})	Δc^a ($\times 10^{13}$ spins cm^{-2})
373		5.6 ± 0.8	−2.8 (24 h)
473		62 ± 4	−2.0 (7 h)
	0.3 ± 0.2	45 ± 7	−0.7 (69 h)
523	2.0 ± 0.5		3.3 (18 h)
	2.3 ± 0.1		4.2 (123 h)
573	9 ± 1		4.3 (5 h)
	16 ± 2		4.9 (6 h)
613	30 ± 8		5.6 (8 h)

[a] Samples underwent exposures of different duration (parentheses).

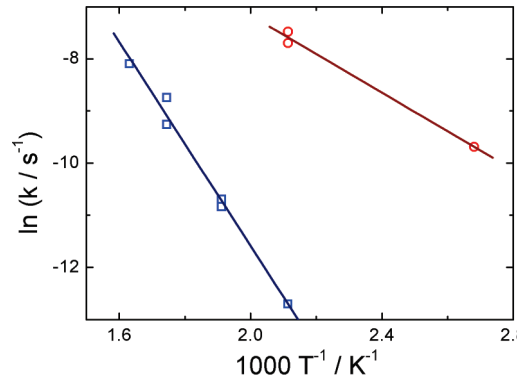

FIGURE 4. Arrhenius plots for the stabilization (○) and degradation (□) processes found in the thermal degradation of Kapton HN.

It appears evident from the recorded data that at least two competing mechanisms are present. One is dominating at higher temperatures, causing radical generation, and a second dominates at lower temperatures leading to a stabilization of the material by radical termination.

From the temperature dependent rate constants Arrhenius plots as shown in Figure 4 were made, arriving at apparent activation energies of (81 ± 12) kJ mol^{-1} and (31 ± 22) kJ mol^{-1} for the degradation and stabilization processes, respectively.

UV Degradation. Irradiation of the polyimides showed that they could not withstand the full light intensity provided by the lamp. Because of the size of the optical window of the ESR resonator, only a small part of the films received the irradiation and the materials were scorched, and in some cases the light burned completely through them. Therefore, a filter was used, reducing the light intensity to approximately 40% (14). Note that FEP-C was so UV sensitive that a second filter had to be installed (reduction to 16%).

Table 2. Average Experimental Rate Constants and Changes in Radical Concentrations (Δc) of UV-Induced Degradation Reactions

material	k_3 ($\times 10^{-2}$ s^{-1})	k_4 ($\times 10^{-4}$ s^{-1})	Δc ($\times 10^{15}$ spins cm^{-2})
Kapton HN (25 μm)	1.5 ± 0.4	5.9 ± 0.9	1.5
Kapton HN (50 μm)	1.1 ± 0.4	10 ± 2	1.6
Kapton HN (75 μm)	1.8 ± 0.7	7 ± 1	1.5
Upilex S (25 μm)	1.7 ± 0.4	22 ± 3	2.6
Upilex RN (25 μm)	1.1 ± 0.6	20 ± 7	1.1
FEP-C (25 μm)	0.9 ± 0.1	5 ± 1	2.4

However, even with these filters, a light brownish discoloration of the materials was observable after the exposure. It was shown by Iwata (6) that this correlates well with the amount of radicals generated in the material. The area of the discoloration was used for calculation of spin concentrations, cf. Table 2, and was on average 0.3 cm^2.

At the reduced light intensity, it was possible to obtain curves as shown in Figure 5, where the corrected double integral, $A(t)-A(0)$, is plotted as a function of time; as can be seen, the behaviors of the four materials were very similar. Additional kinetic traces are given in the Supporting Information.

The data obtained in the experiments were analyzed using different kinetic functions and it was found that a simple exponential increase no longer offers a sufficient description. Instead, a biexponential one was used and it fits the data reasonably well. This indicates that at least two degradation reactions take place simultaneously, possibly leading to the formation of different radicals. The faster of the two processes corresponded to a rate constants of $k_3 \approx 10^{-2}$ s^{-1}, whereas the slower had $k_4 \approx 10^{-4}$ s^{-1}, cf. Table 2 for details. Note that for Kapton HN, the rate constant of the slow process is similar to those seen in Table 1, indicating a possible thermal degradation taking place because of heating of the sample caused by the UV irradiation.

Judging from the amount of radical generated in the samples, Kapton HN and Upilex RN exhibit the highest UV stability of the materials. Not surprisingly, FEP-C is the least stable, showing almost the same spin concentration as Upilex S, albeit receiving 60% less radiation.

From the experiments conducted on the 25, 50, and 75 μm Kapton HN films it is seen that both kinetics and the amount of UV generated radicals are independent of the film thickness. Thus the radicals must be situated very near the surface of the film. This is in good accord with the results of George et al. (6) who also report a spin concentration of 1.85 $\times 10^{17}$ spins g^{-1} after UV irradiation of 20 μm Kapton H films (200W, 1 h). This corresponds to an increase of 1.1 $\times 10^{17}$ spins g^{-1} as compared to 3.2 $\times 10^{17}$ spins g^{-1} (1.5$\times 10^{17}$ spins cm^{-2}) for the 25 μm film investigated here. The relatively large disagreement is attributable to differences in experimental conditions, with the most important one being that the literature value is from ex situ irradiated films.

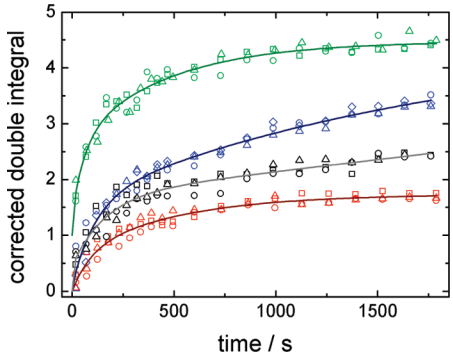

FIGURE 5. Kinetic traces for UV irradiated Upilex S, FEP-C, Kapton HN, and Upilex RN (top to bottom).

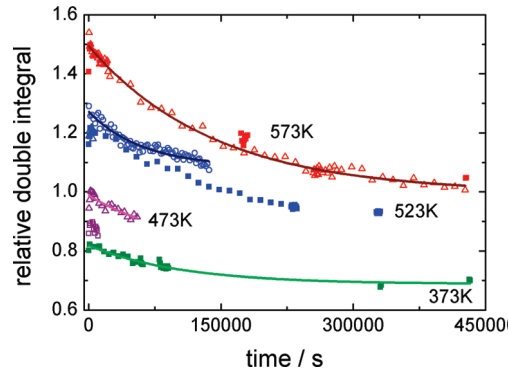

FIGURE 6. Stability of thermally generated radicals in Kapton HN after exposure to air. Data correspond to spectra acquired at 298 K of samples that were originally exposed to elevated temperatures. Closed symbols denote samples that were handled and open symbols those that were kept inside the ESR cell.

Stability of Exposed Samples. At the end of several experiments, the stability of the radicals generated through UV or elevated temperature exposure was monitored. Samples remained in the ESR spectrometer under continuous evacuation, typically for 15–40 h, while spectra were acquired at appropriate intervals. During this, only a slight decrease in radical concentration, at most 5%, could be observed.

After this, the ESR cell was vented and remained inside the spectrometer while regular ESR spectra were recorded. This procedure went on for as long as a week and simple exponential decays of the radicals were observed. The associated rate constants were of the order of 10^{-5} s^{-1}, corresponding to a half-life of approximately 15–25 h. This is in good agreement with a previous report (6), which found that electron irradiated samples of Upilex S show a complete depletion of radiation generated radicals after 100 h. This report also identified oxygen as the main reason for the radical decay, as it can permeate into the polymer and destroy the radicals.

For comparison, some samples were "handled", i.e. removed from the sample cell after monitoring the initial decay and subsequently stored for weeks and during this time occasionally reintroduced to the ESR spectrometer for further measurements. Table S2 in the Supporting Information shows the observed rate constants of the decay.

Kinetic traces for the decay of radicals in the thermally treated Kapton HN samples are shown in Figure 6. These originate from spectra recorded at 298 K and again the relative double integral has been plotted, with the normal-

ization corresponding to spectra acquired at 298 K prior to the thermal exposure. The reason that the data from samples that have experienced the same elevated temperature do not always coincide is that the time of exposure varied, cf. Table 1. It is interesting to note that the signal decay is observed even for the samples where the stabilization reaction could be observed. For instance, the sample that was kept at 373 K showed a signal reduction to approximately 80% of the initial value after heating. During the monitoring of the sample in air, the signal dropped to less than 70% after 125 h. This is evidence that even at this relatively low temperature degradation has taken place. The radicals resulting from this process decay in a similar fashion as those resulting from higher temperatures. In contrast, there is no evidence of reformation of radicals that had been eliminated in the stabilization process.

From these investigations, it is clear that some care must be taken when comparing results obtained from different sources. If ex situ degradation methods have been applied, one must expect lower radical concentrations and different kinetics. However, as the ESR spectra did not change significantly during storage, interpretations based on single spectra taken at any stage should serve equally well. Furthermore, from Figure 6, it can be seen that laboratory handling and the type of storage in air do not affect the decay of the ESR signal.

CONCLUSIONS

Using the newly setup ESR facility, it was possible to gain new insights in the processes that take place during the thermal and UV degradation of polymers.

The thermal degradation experiments on Kapton HN revealed a very interesting temperature dependence of the reaction kinetics. It is clear that two processes take place during the heating of the samples. At low temperatures, a stabilization of the material was observed, whereas at high temperatures, degradation took place. In the intermediate region, both processes could be detected.

From the UV irradiated samples, it was shown that the degradation kinetics are quite similar for the four materials. Biexponential decays were found, indicating a more complex degradation mechanism. The amounts of radicals generated during the irradiation process varied between the samples and the most stable materials were Upilex RN and Kapton HN. FEP-C was the least stable, showing only slightly less radicals than Upilex S, but at 60% lower irradiation intensity. Furthermore, it was confirmed that the radicals are created mainly at the surface of the film.

The UV-generated radicals are quite stable in a vacuum, under continuous evacuation, but disappear with a half-life of about 20 h when exposed to air. This illustrates the importance of in situ measurements when concerned with space environment simulations. Storage and handling did not affect the decay.

Within a family of similar materials, a relative comparison for materials performance was possible; however, with the current method, it is not yet possible to gain absolute performance characteristics of materials. Future challenges involve a better consideration of effected volume within the material, the formation of gradients, and the isolation of radical species that may contribute to different extent to the subsequent degradation reactions.

Acknowledgment. The authors thank the European Space Agency (Networking/Partnering Initiative) and the county of Styria, Department of Science and Research, for financial support.

Supporting Information Available: Tables with additional ESR data and rate constants for the decay of the Kapton HN ESR signal in air as well as figures with ESR spectra and kinetic traces (PDF). This material is available free of charge via the Internet at http://pubs.acs.org.

REFERENCES AND NOTES

(1) Weil, J. A.; Bolton, J. R.; Wertz, J. E. *Electron Paramagnetic Resonance, Elementary Theory and Practical Applications*; Wiley-Interscience, New York, 1994.
(2) Yordanov, N. D. *Appl. Magn. Reson.* **1994**, *6*, 241–257.
(3) Ahn, M. K.; Weber, R. T.; Meador, M. A. *NASA Conf. Publ.* **1993**, *19117*, 20/1–20/11.
(4) Ahn, M. K.; Stringfellow, T. C.; Fasano, M.; Bowles, K. J.; Meador, M. A. *J. Polym. Sci., Part B: Polym. Phys.* **1993**, *31*, 831–841.
(5) Ahn, M. K.; Eaton, S. S.; Eaton, G. R.; Meador, M. A. *Macromolecules* **1997**, *30*, 8318–8321.
(6) Iwata, M. *Proceedings of the 10th ISMSE & 8th ICPMSE*; Collioure, France, June 19—23, 2006; European Space Agency: Paris, 2006; ESA SP-616.
(7) George, M. A.; Ramakrishna, B. L.; Glausinger, W. S. *J. Phys. Chem.* **1990**, *94*, 5159–5164.
(8) Zhdanov, G. S.; Klinshpont, E. R.; Iskakov, L. I. *Nucl. Instrum. Methods Phys. Res., Sect.B* **2001**, *185*, 140–146.
(9) Devasahayam, S.; Hill, D. J. T.; Connell, J. W. *Radiat. Phys. Chem.* **2001**, *62*, 189–194.
(10) Artiaga, R.; Chipara, M.; Stephens, C. P.; Benson, R. S. *Nucl. Instrum Methods Phys. Res., Sect.B* **2005**, *236*, 432–436.
(11) Iwata, M.; Imai, F.; Imagawa, K.; Morishita, N.; Kamiya, T. *Proceedings of the 9th ISMSE*; Noordwijk, The Netherlands, June 16—20, 2003; European Space Agenecy: Paris, 2003; ESA SP-540, pp 617—621.
(12) Popok, V. N.; Azarko, I. I.; Khaibullin, R. I.; Stepanov, A. L.; Hnatowicz, V.; Mackova, A.; Prasalovich, S. V. *Appl. Phys. A: Mater. Sci. Process.* **2004**, *78*, 1067–1072.
(13) Hill, D. J. T.; Rasoul, F. A.; Forsythe, J. S.; O'donnell, J. H.; Pomery, P. J.; George, G. A.; Young, P. R.; Connell, J. W. *J. Appl. Polym. Sci.* **1995**, *58*, 1847–1856.
(14) Rasmussen, K.; Grampp, G.; van Eesbeek, M.; Rohr, T. *Proceedings of the 11th ISMSE*; Aix en Provence, France, Sept 15—18, 2009; European Space Agency: Paris, 2009; published online at http://esmat.esa.int
(15) Duling, D. R. *J. Magn. Reson., Ser. B* **1994**, *104*, 105–110.
(16) Hill, D. J. T.; Mohajerani, S.; Pomery, P. J.; Whittaker, A. K. *Radiat. Phys. Chem.* **2000**, *59*, 295–302.
(17) Semprimoschnig, C. O. A.; Heltzel, S.; Polsak, A.; van Eesbeek, M. *Proceedings of the 9th ISMSE*; Noordwijk, The Netherlands, June 16—20, 2003; European Space Agenecy: Paris, 2003; ESA SP-540, pp 161—167.
(18) Heltzel, S.; Semprimoschnig, C. O. A. *Proceedings of the 9th ISMSE* **2003**, 179–185, ESA SP-540.

AM100219Z